Infrared free-electron laser photoablation of diamond films

Judit Sturmann, Z. Marka, M. M. Albert, Royal G. Albridge, Jonathan M. Gilligan, et al.

Judit Sturmann, Z. Marka, M. M. Albert, Royal G. Albridge, Jonathan M. Gilligan, Gunter Luepke, S. K. Singh, Jeffrey L. Davidson, Wolfgang Husinsky, Norman H. Tolk, "Infrared free-electron laser photoablation of diamond films," Proc. SPIE 4423, Nonresonant Laser-Matter Interaction (NLMI-10), (26 June 2001); doi: 10.1117/12.431224

SPIE.

Event: Nonresonant Laser-Matter Interaction (NLMI-10), 2000, St. Petersburg, Russian Federation

Infrared free-electron laser photo-ablation of diamond films

J. Sturmann[a], Z. Marka[a], M. M. Albert[a], R. G. Albridge[a], J. M. Gilligan[a], G. Lüpke[a], S. K. Singh[a], J. L. Davidson[b], W. Husinsky[c] and N. H. Tolk[a]

[a]Department of Physics and Astronomy, Vanderbilt University, Nashville, TN 37235
[b]Department of Electrical Engineering, Vanderbilt University, Nashville, TN 37235
[c]Institut für Allgemeine Physik, Technische Universität Wien, Austria

ABSTRACT

We report first infrared free-electron laser experiments to compare and elucidate the effects of surface-localized vibrational excitation versus bulk vibrational excitation on the ablation of polycrystalline diamond. The measured ablation yield values as a function of laser intensity indicate the existence of two separate thresholds. The lower intensity threshold is identified as the ablation threshold, and the higher intensity threshold is associated with the formation of a plasma plume. The wavelength dependences of both thresholds indicate that the C-H absorption occurring at surfaces and grain boundaries does not play a significant role in the ablation process. However, both thresholds are lower when the laser is resonant with the two-phonon bulk absorption band. These findings are consistent with the model that a rapid laser-induced phase transition to graphite is responsible for the low-intensity ablation of diamond at and above the first threshold.

Keywords: photo-ablation, free-electron laser, phase-transition, diamond, vibrational excitations, impurities, and semiconductors

1. INTRODUCTION

Most infrared laser ablation experiments are performed with Nd:YAG or CO_2 lasers, confining the studies to 1.064 μm and 10.6 μm wavelengths respectively. Free-electron lasers (FEL), unlike conventional lasers, convert the kinetic energy of free relativistic electrons into radiation instead of relying on electron transitions between two bound-state energy levels in an active medium. FELs have the broadest tuning range of all types of lasers and are capable of high power output. The FEL at Vanderbilt University provides a unique opportunity for laser ablation studies in the 2-10 μm region. This wide range tunability makes it possible to perform systematic wavelength-dependent studies of photo-ablation on materials.

IR laser ablation experiments on diamond films offer an excellent opportunity to investigate energy localization in ablation. CVD (chemical vapor deposition) diamond films have two distinct absorption bands close to each other in the spectral region available to us: one represents bulk absorption, the other surface absorption due to hydrogen. The broad two-phonon band peaks around 5μm, while the vibrational band of the adsorbed hydrogen on surfaces peaks around 3.5 μm. In a CVD diamond film, the absorption coefficient is about 9 cm^{-1} both at 3.5 and 5 μm wavelength. The absorption is weak in both of these absorption bands. In addition, diamond is a very good heat conductor at room temperature. Up to now, no experiment has been done to test the wavelength-dependence of ablation in the range 3 to 5.5 μm. With the choice of this wavelength range for diamond ablation, it is possible to learn whether the resonant excitation of surface-localized hydrogen influences significantly the ablation process compared to resonant bulk excitations.

In laser ablation near the threshold, the energy is delivered to a very small volume of the target material. The laser provides an initial high concentration of energy, but the absorbed energy must remain spatially localized for a sufficient time in order to cause bond breaking and vaporization. A key issue is to understand how is it possible to localize sufficient absorbed energy in various materials. The earliest models for laser ablation focused on the thermal character of ablation. The assumption of vaporization at normal boiling temperature fits the data only of long-pulse (in the order of several hundred microseconds) metal [1] and graphite [2] ablation experiments below the GW/cm^2 intensity range. In ablation with shorter laser pulses in the GW/cm^2 intensity regime, the role of thermal pressure [3] and shock waves [4] in the target material has also been taken into consideration in theoretical treatments. However, the simple thermal model has proven inadequate [5]. Experiments with tungsten and aluminum show that adsorbates can localize the otherwise delocalized excitation of conduction electrons and this way lower the threshold for ion ejection [6].

In many cases, structural modification accompanies ablation. Reif and coworkers [7, 8] first proposed an alternative ablation model based on defect accumulation during the laser pulse. The basic idea in their model is that, as defects accumulate during the laser pulse, a large density of unoccupied surface electronic states could be reached by multi-photon

Nonresonant Laser-Matter Interaction (NLMI-10), Mikhail N. Libenson, Editor
Proceedings of SPIE Vol. 4423 (2001) © 2001 SPIE · 0277-786X/01/$15.00

transitions. A sufficient number of electron-hole pairs could be created. Relaxation of electron-hole pairs to localized excited states could lead to bond breaking through non-radiative transitions. Phase transitions have been shown to be involved in many cases of laser ablation. The most trivial case of that is the melting of metals. The diamond to graphite phase change, induced by near but below bandgap KrF laser (5.0 eV) radiation, was observed before the evaporation of diamond films [9]. Both the rate and threshold of evaporation are related to the purity of the diamond films: the purer the films, the higher the thresholds and the lower the evaporation rates. The classical phase transformation theory is usually not applicable to laser irradiation. The high heating and cooling rates due to the spatial and temporal locality of laser radiation require modification of the classical thermodynamic theory of phase transformation [10].

In this paper we describe wavelength-dependent photo-ablation studies of CVD diamond films in the infrared region. Comparision of ablation thresholds at a surface (C-H stretch) and a bulk (two-phonon) absorption features indicate that the ultimate ablation mechanism is the same for localized and delocalized initial excitations. At all wavelengths, two threshold-like increases in the positive ion yield were found as a function of laser intensity. The first threshold corresponded to the onset of large-scale positive ion ejection (ablation threshold), and the second increase of ion yield coincided with the appearance of UV luminescence, which is attributed to the formation of a plasma plume (plasma threshold). Our experimental data suggests that the onset of photo-ablation at the first threshold is initialized by explosive phase transition from diamond to graphite.

2. EXPERIMENT

The experiments were carried out at the W.M. Keck Free-Electron Laser Center at Vanderbilt University. This free-electron laser [11,12] is capable of operating at wavelengths from 2 μm to 9.8 μm. The typical repetition rate is 30 Hz, the IR macro-pulse energy is around 50 mJ, and the length of the IR pulse is between 2-6 μs. Each macro-pulse consists of 1 ps micro-pulses spaced at intervals of 350 ps. The peak power in a micro-pulse is usually around 6-8 MW, but it can reach 10-20 MW.

For the detection of the ablated particles, a time of flight (TOF) apparatus was used without extraction voltage (Figure 1). The TOF consisted of a detector and a drift tube. In a laser ablation event, both positive and negative ions along with neutral particles are ejected into the gas phase. The experiment was set up to detect positively charged particles among the ablated material. No post-ionization was applied. In order to preserve original velocities, no accelerating field was used, except in auxiliary experiments to estimate kinetic energies. In the TOF apparatus the detector was a chevron assembly of a pair of microchannel plates (MCP) fitted with a co-axial anode. The detector was biased to detect positive ions. The front surface of the chevron was maintained at –2000 V, the rear surface at –200 V, and the anode was at ground potential. Channel plates have direct sensitivity to charged particles and energetic photons. The work function of the channel plates allow photoelectron production at incident photons having wavelengths shorter than 200 nm (6.2 eV). The drift tube is positioned at a port of the ultra-high vacuum (UHV) chamber at 45-degree angle to the sample normal. The end of the drift tube is at 54 cm from the center of the UHV chamber, where the sample was mounted. The vacuum was maintained in the low 10^{-9} Torr range.

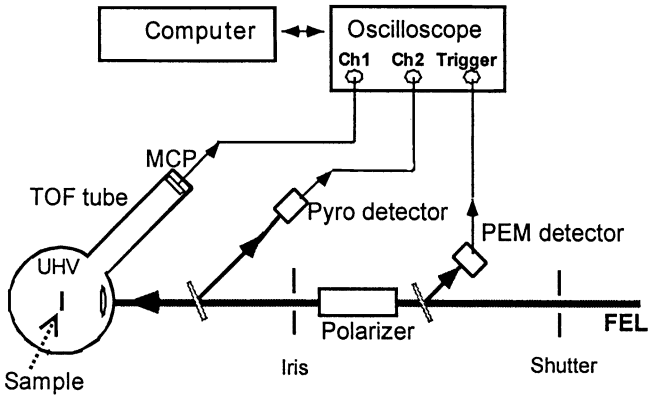

Figure 1 Experimental setup

In order to allow sufficient time for the sample to cool between macro-pulse shots, single macro-pulses were gated out from a given FEL pulse train. In the experiments, the laser spot size and the beam attenuation had to be precisely controlled. The beam intensity incident on the sample was varied using a ZnSe Brewster-plate polarizer. Because of fluctuation in the macro-pulse energy, the energy of each macro-pulse was measured. To filter out higher harmonics, a pair of Ge plates mounted at Brewster's angle was placed in the beam. A single plano-convex CaF_2 lens was located inside the UHV chamber which was used to focus the laser beam onto the sample with a laser beam spot size of 75 μm. In order to ensure spot-size uniformity at different wavelengths the dispersion in CaF_2 was taken into account.

The TOF spectrum of ejected positive ions and the energy of the corresponding laser macro-pulse were recorded simultaneously with a digitizing oscilloscope. Each TOF signal was recorded for 500 μs with a 1 μs resolution. In the TOF spectra t=0 represents the arrival of the leading edge of the macro-pulse to the sample. A fast IR photo-electromagnetic (PEM) detector was used to generate a trigger for the oscilloscope from a small portion of the laser pulse. The energy of the

laser macro-pulses was monitored using another small portion of the beam by a pyroelectric joulemeter. After each change in wavelength the joulemeter was calibrated against a calorimeter. During calibration, the calorimeter was positioned directly in front of the UHV chamber window. To calculate laser power in a micro-pulse, the temporal profile of an average macro-pulse was used. The laser beam is characterized in this paper by its wavelength and peak intensity. The peak intensity is defined as the intensity at the center of a Gaussian laser beam during a micro-pulse.

The samples used in these experiments were polycrystalline intrinsic diamond films, approximately 10 μm thick, deposited on a 500 μm thick silicon substrate. The films were grown using the microwave plasma-assisted chemical vapor-deposition (CVD) process [13]. The grain size in the top layer is typically smaller than 0.5 micron. Fourier transform infrared (FTIR) spectra taken on the samples show the typical features of CVD diamond films. Figure 2 shows the absorption of one representative sample in the studied spectral range. The hydrogen content of the film was high enough to make the C-H vibrational absorption maximum equal to the maximum of the two-phonon absorption. The absorption coefficient is small in this spectral range, such that a film of 10-μm thickness absorbs less than 2% of the incident radiation.

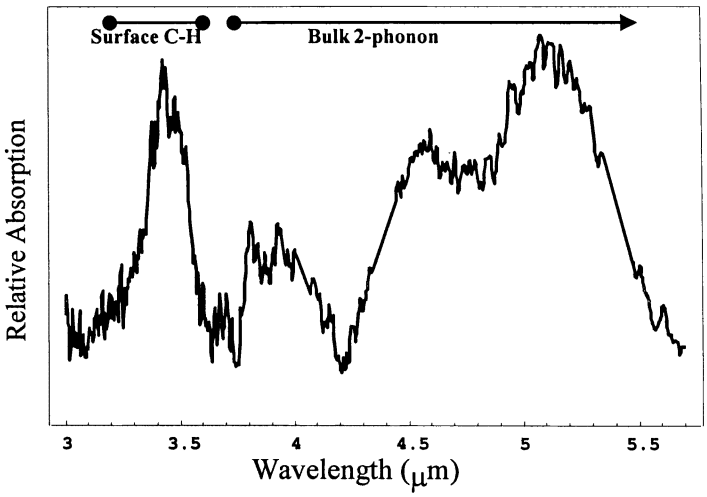

Figure 2 FTIR spectrum of one repesentative CVD diamond film sample in the studied wavelength range

3. RESULTS

Figure 3 shows time-of-flight spectra at a given laser intensity just barely above the first ablation threshold, where several macro-pulses were incident on the same spot on the sample. The time span between shots was 7-12 seconds, long enough to avoid heat buildup from previous macro-pulses. This series of TOF spectra obtained by repeated FEL macro-pulse shots shows that the diamond target was gradually modified by the laser irradiation. After 10-20 shots on the same spot, the peaks vanished indicating the removal of the film from the substrate. In this case carbon atoms are removed at a rate of few thousand layers per macro-pulse. Above a certain laser intensity corresponding to the second observed threshold, in addition to the two delayed peaks shown in Figure 3 a prompt MCP signal was observed. The leading edge of this peak was within the first 1-3 μs. We attribute this prompt peak to UV photons generated in the ablation plume associated with conventional ablation.

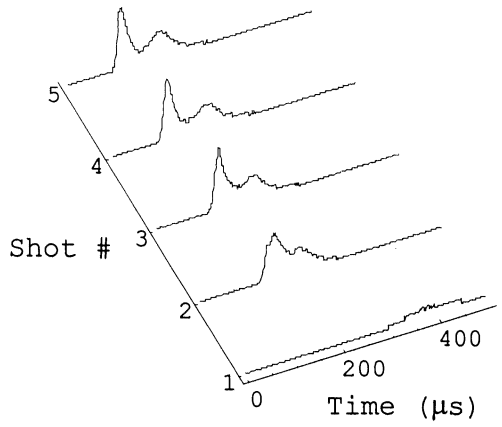

Figure 3 Time of flight spectra for repeated macropulse shots on the same spot slightly above the ablation threshold. The spot diameter was 150 μm, the wavelength was 3.5 μm.

Figure 4 shows a typical example of the integrated ablation yield of positive ions as a function of laser micro-pulse intensity. The arrow marks those intensities where UV photons were also emitted. Notably, the onset of UV luminescence corresponds to a second rise in the yield of positive ions. These plots show the existence of two thresholds at all probed wavelengths. Above the ablation threshold, which is the lower intensity threshold of the two observed thresholds, there is a nearly constant ablation yield over a broad range of intensities. As the intensity increases, a second threshold, the plasma threshold, is observed. At the plasma threshold intensity, a prompt signal appears which we attribute to UV arising from an ablation induced plasma plume. Above the plasma threshold intensity, a second increase of ion yield is observed with increasing laser intensity.

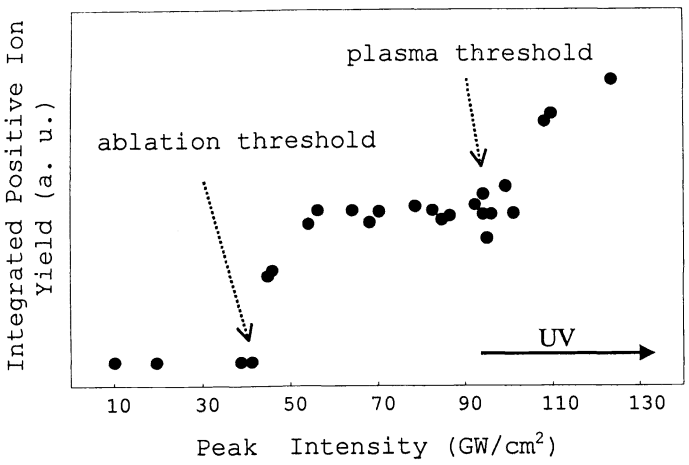

Figure 4 Typical example of positive ion yield as a function of peak laser intensity. These are first macro-pulse shot data taken at 3.9 μm with a spot diameter of 75 μm. The arrow indicates the intensities where UV photons are also emitted.

Preliminary experiments were carried out with a – 200 V acceleration voltage applied to the drift tube. This value was chosen as a compromise since the 2-6 μs length of the macropulse strongly limits our mass/charge resolution. These TOF spectra indicate the formation of C_2 and C_3 clusters and also show that the size distribution of ablated particles has a tail that extends to several tens of carbon atoms per electron charge. In addition, we performed experiments at varying retarding potentials. These experiments prove that the kinetic energies of ablated particles reach 200 eV for laser intensities between the first and second thresholds.

Ablation thresholds and plasma thresholds were determined at several wavelengths. Figure 5 displays the ablation and plasma thresholds as a function of wavelength determined from first and second macro-pulse shots. The wavelength dependence of ablation thresholds generally follows the two-phonon absorption spectrum. Both the ablation and plasma thresholds have a minimum, which coincides with the bulk 2-phonon absorption maximum of the diamond film. Even though the C-H absorption is comparable in magnitude to the 2-phonon absorption, there is no significant reduction in threshold intensities in the region of the C-H absorption peak. By comparing first-shot and second-shot ablation thresholds one finds that second-shot ablation thresholds are slightly lower, and they still reflect the 2-phonon absorption spectrum. In contrast, a significant reduction in the plasma thresholds for the second shots is observed, especially at shorter wavelengths outside the phonon absorption band. Lower second-shot thresholds suggest defect creation or material modification.

4. DISCUSSION

Our data demonstrate the existence of two distinct ablation thresholds for the case of IR diamond ablation. In addition to the first ablation threshold, another threshold, which we associate with plasma-dominated ablation, is observed. At the first ablation threshold intensity there is a steep rise in the ablation yield as laser intensity increases which then remains constant until the onset of plasma dominated ablation. We estimate that in the region between the two ablation thresholds the material removal rate is of the order of thousand monolayers per macro-pulse shot. We have demonstrated that among the ablated material, there are ion clusters consisting of tens of carbon atoms.

The wavelength dependence of ablation thresholds reflects lower thresholds in the two-phonon absorption band. There is no reduction of thresholds, however, in the C-H absorption band despite of the similar low intensity absorption. This suggests that the hydrogen on the surface does not play a significant role in the actual ablation process. C-H vibrations do not couple well to the bulk. It is likely that the spectral bandwidth of the FEL makes vibrational up pumping possible, and hydrogen is removed from the surface even below the temperature required for thermal desorption when irradiated with resonant FEL photons.

The experimental results provide evidence for the modification of sample properties as a result of laser irradiation. TOF spectra of consecutive shots on the same spot on the sample (Figure 3) demonstrate that repeated FEL macro-pulse shots cause gradual changes in the sample. The changes in TOF spectra suggest accumulation of defects and structural imperfections in the CVD diamond film due to prolonged exposure. Gruzdev and Libenson showed that the electric field could be strongly localized at defect sites. Intensity dependent changes in the refractive index of inclusion and host lead to extremely high local amplitudes of the electric field [14]. This involves a threshold behavior for the absorption that cannot be anticipated from the linear absorption properties. All these changes may increase the absorption by orders of magnitude. The absorbed portion of the laser energy may reach a sufficiently high percentage, which is enough to raise the local temperature at the irradiated spot to a point when the diamond begins to graphitize. Earlier experiments indicate that graphitization of diamond accompanies UV [9, 15] as well as IR ablation [16]. Micro-Raman spectra versus number of macropulse shots taken around the ablation crater for our samples show the dramatic decrease in the diamond peak at 1332 cm^{-1} and the appearance of pronounced graphite signatures at 1580 cm^{-1} and 1350 cm^{-1}.

Above ablation threshold as laser intensity increases, the ejected neutral and charged particles form an increasingly denser cloud above the target surface, and the fraction of ionized particles also increases indicated by the rapidly increasing ion yield (Fig. 3). After the first sharp rise, measured yield intensity curves reach a saturation level. Here the ejected particle cloud reaches a density where the increasing laser intensity contributes more to the increased heating of the particle cloud than to the removal of more material from the sample.

We observed a second increase of the ion yield above the plasma threshold intensity, i.e. the intensity at which UV luminescence appeared in the TOF spectra. We believe that the UV luminescence is the indication of the formation of ablation plasma. The ablation plasma plume can almost completely absorb the incoming IR energy, and convert the absorbed IR energy into visible and UV radiation and into increased kinetic energies of the electrons and ions. The sample is now irradiated by more energetic photons allowing electronic transitions even in the not yet graphitized layers in the sample. These newly opened energy channels make possible the observed increased ablation yields.

In our case, a phase change to graphite is more likely than melting during diamond ablation, since the melting of diamond occurs above the temperature of 3000 K well below what we have calculated for the temperature increase of our irradiated volume [17]. On the other hand, diamond, which is metastable at low pressures, can turn into graphite by overcoming a relatively small activation barrier. The activation energy was measured to be 1.95 eV plus or minus 0.3 eV by Kuznetsov et al. when the diamond was heated in vacuum [18]. However, computer simulations of damage in diamond due to ion impact and its annealing by Saada and coworkers showed that if the vacancy density is sufficient, the activation energy of graphitization can be as low as 0.7eV [19]. In UHV conditions uncatalyzed graphitization occurs at 1800K [20], which is much lower than the melting temperature. Defect-catalyzed graphitization may occur at an even lower temperature of 1100K [21].

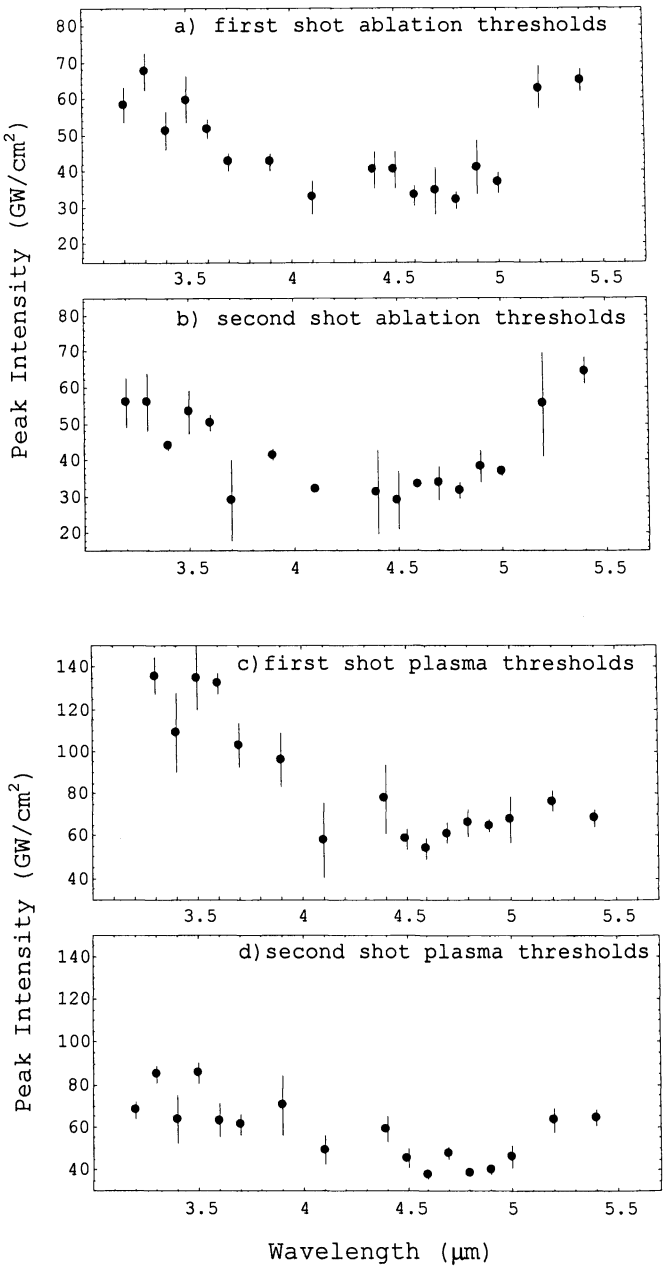

Figure 5 First (a) and second shot ablation thresholds (b) and first (c) and second shot plasma thresholds (d) for a CVD diamond film as a function of wavelength. The diameter of irradiated spot is 75 μm.

We propose a model for IR laser ablation of diamond in which the ablation threshold is related to the threshold for phase transition to graphite. Graphitization may be explained in two ways. One possibility is that the FEL radiation causes non-thermal graphitization. Diamond may overcome the activation barrier by multi-photon absorption of the infrared FEL radiation. However, these experiments provide no evidence for major involvement of a multi-photon process. The other possibility is that the absorption coefficient of CVD diamond changes significantly during an intense FEL macro-pulse, and thereby the local temperature may reach sufficient values for thermal graphitization. It is likely that the intense FEL irradiation creates more defects and changes the electronic and optical properties of the diamond film consequently. The accumulation of defects, in other words gradual change in electronic properties, is supported by the observed evolution of TOF spectra shapes of repeated macro-pulses near the ablation threshold. As soon as graphite regions

are formed, further enhancement of absorption takes place by free carriers in the conduction band of graphite. As a result of the intense laser radiation the graphite phase can progress at a higher rate into the bulk of the diamond than the rate of graphitization due to conventional heating.

If the diamond changes into graphite phase before ablation, a large mechanical stress is created simply due to the density difference of the two phases. Because of its smaller density, graphite occupies roughly 1.5 times the volume of diamond with similar mass. The mechanical stress could lead to the cracking and spallation of the graphite layer. The rapid progression of the graphite phase can result in violent ejection of large clusters due to the rapid volume expansion. This ejection mechanism is similar to the popping of popcorn. At the threshold intensity, *explosive graphitization* may occur in a small central region of the laser spot near the end of the FEL macro-pulse. This explosive process can lead to very high ion kinetic energies as observed in the retarding potential experiments. At only slightly higher laser intensity, the graphitized volume can increase drastically because of the drastic change in absorption properties as a consequence of the largely different electronic properties of graphite compared to diamond.

5. CONCLUSION

We described here the first investigation of CVD diamond film ablation in the IR wavelength range of 3-5.4μm. Measured ablation yields as a function of laser intensity indicate the existence of two separate thresholds in case of CVD diamond ablation. The lower threshold intensity is identified as ablation threshold, and the higher threshold intensity is the plasma threshold. Both thresholds have their lowest values when the initial excitation is delocalized bulk two-phonon absorption. The adsorbed hydrogen on the surfaces of the diamond film does not lower the ablation threshold. The evolution of TOF spectra as a result of repeated FEL macro-pulse shots indicates the involvement of laser-induced material modification. Based on our findings we propose that explosive phase transition to graphite leads to the ablation of diamond in the IR region.

6. ACKNOWLEDGMENTS

The authors would like to thank the effort of the staff of the W.M. Keck Free-Electron Laser Center. This project was supported by the Office of Naval Research.

7. REFERENCES

1. V. B. Braginskii, I. I. Minakova and V. N. Rudenko, *Sov. Phys. Tech. Phys. 12*. 753 (1967).
2. P. D. Zavistanos, *GE Rep.* R67SD11 (1967).
3. Y. V. Afanasev and O. N. Krokhin, *Sov. Phys. JETP 25*, 639 (1967).
4. S. S. Penner and O. P. Sharma, *J. Appl. Phys. 37*, 2304 (1966).
5. R. V. Dreyfus, R. Kelly and R. E. Walkup, *Appl. Phys. Lett. 49*, 1478 (1986).
6. H. S. Kim and H. Helvajian, *J. Phys. Chem. 95*, 6623 (1991).
7. J. Reif, H. Fallgren, W. E. Cooke, E. Matthias, *Appl. Phys. Lett. 49*, 770 (1986).
8. J. Reif, H. Fallgren, H. B. Nielsen, E. Matthias, *Appl. Phys. Lett. 49*, 930 (1986).
9. A. Blatter, U. Bögli, L. L. Bouilov, N. I. Chapliev, V. I. Konov, S. M. Pimenov, A. A. Smolin and I. V. Spitsyn, *Proc. of the Second Int. Symp. On Diamond Materials, Vol. 91-8*, 351 (1991).
10. E. N. Sobol, *Phase Transformations and Ablation in Laser-Treated Solids*, Wiley, 1995.
11. C. A. Brau, *Nucl. Instr. and Meth. in Phys. Res., A 318*, 38 (1992).
12. G. S. Edwards, D. Evertson, W. Gabella, R. Grant, T. L. King, J. Kozub, M. Mendenhall, J. Shen, R. Shores, S. Storms and R. H. Traeger, *IEEE J. Sel. Topics Quantum Electron. 2*, 810 (1996).
13. W. Zhu, B. R. Stoner, B. E. Williams and J. T. Glass, *Proceedings of the IEEE, 79(5)*, 621 (1991).
14. V. E. Gruzdev an M. N. Libenson, *Laser Damage in Optical Materials: 1994, SPIE Proc. 2428*, 553 (1995).
15. M. Rothschild, C. Arnone and D. J. Erlich, *J. Vac. Sci. Technol. B 4*, 310 (1986).
16. A. Ueda, *Ph. D. Dissertation, Vanderbilt University*, Nashville, TN, 1994.
17. J. Sturmann, *Ph. D. Dissertation, Vanderbilt University*, Nashville, TN, 1999.
18. V. L. Kuznetsov, I. L. Zilberberg, Y. V. Butenko, A. L. Chuvilin and B. Segall, *J. Appl. Phys. 86*, 863 (1999).
19. D. Saada, J. Adler and R. Kalish, *Phys. Rev. B 59*, 6650 (1999).
20. T. Evans, in *Properties of Diamond* Ed. J. E. Field, p.403, Academic Press, UK, 1979.
21. G. S. Woods, *Ph. D. Thesis, University of the Witwatersrand*, South Africa, 1971.